

Multi-periodic climate dynamics: spectral analysis of long-term instrumental and proxy temperature records

H.-J. Lüdecke^{1,*}, A. Hempelmann², and C. O. Weiss^{3,*}

¹HTW, University of applied sciences, Saarbrücken, Germany

²University of Hamburg, Department of Astronomy, Hamburg, Germany

³Physikalisch Technische Bundesanstalt, Braunschweig, Germany

*retired from

Correspondence to: Lüdecke
(moluedecke@t-online.de)

Abstract. The longest six instrumental temperature records of monthly means reach back maximally to 1757 AD and were recorded in Europe. All six show a V-shape, with temperature drop in the 19th and rise in the 20th century. Proxy temperature time series of Antarctic ice cores show this same characteristic shape, indicating this pattern as a global phenomenon. We used the mean of
5 the 6 instrumental records for analysis by discrete Fourier transformation (DFT), wavelets, and the detrended fluctuation method (DFA). For comparison, a stalagmite record was also analyzed by DFT. The harmonic decomposition of the mean shows only 6 significant frequencies above periods over 30 yr. The Pearson correlation between the mean, smoothed by a 15 yr running average (boxcar) and the reconstruction using the 6 significant frequencies yields $r = 0.961$. This good agreement has a >
10 99.9% confidence level confirmed by Monte Carlo simulations. It shows that the climate dynamics is governed at present by periodic oscillations. We find indications that observed periodicities result from intrinsic dynamics.

1 Introduction

It is widely accepted that the mean surface temperature of the globe has been rising in the 20th cen-
15 tury. However, how strong and how unusual this rise in comparison with the temperature variations over the last 250 or even 2000 yr was is one of the subjects in the actual climate debate. Long-range instrumental records going back to a maximum of about 250 yr BP exist only in Central Europe. But even here they are not abundant. The places with reliable monthly time series number six in all: Prague, Hohenpeissenberg, Kremsmünster, Vienna, Paris and Munich (CRU, 2012; DWD, 2012;
20 Auer et al., 2007; Météo France, 2012; CHMI, 2012). They have some of the longest, most reliable

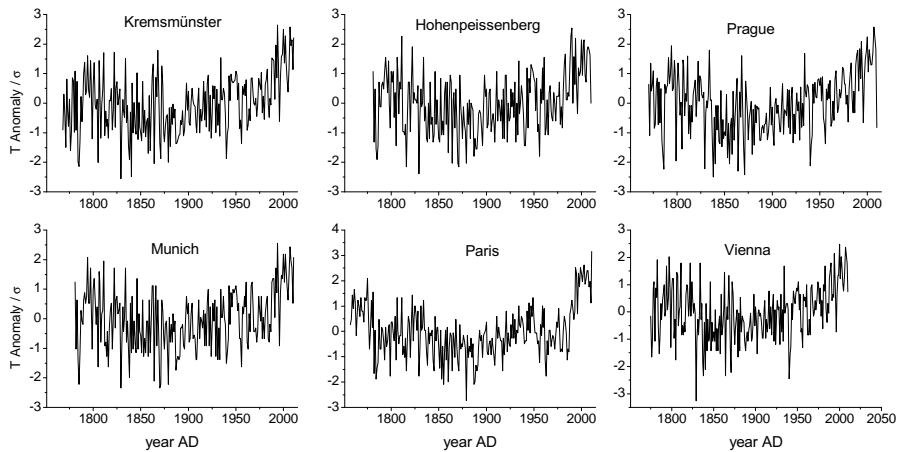


Fig. 1. Long-term temperature records from 6 central European stations

instrumental temperature records as monthly means to be had anywhere. The time series of Paris begins in 1757 AD whereas those of Hohenpeissenberg and Munich begin only in 1781 AD. Additionally, a high quality temperature proxy record from a stalagmite retrieved in the Spannagel Cave near Innsbruck (Austria) at 2347 m.a.s.l. is available ranging from 90 BC until 1935 AD (Mangini et al., 2005). It has time steps between 1 yr and 13 yr. Finally, a yearly $\delta^{18}\text{O}$ record of the period 1801–1997 AD from the analysis of an Antarctic ice core is available for further comparison (Graf et al., 2002).

We used the temperature anomalies divided by the standard deviations for each of the above cited 6 instrumental records from Central Europe. As these are rather close to one another, we used the mean of these (hereafter M6) for the numerical analysis. Equally the anomalies of the stalagmite record and the ice core record, divided by the standard deviations were analyzed (hereafter SPA for the stalagmite record and IC for the ice core record). Figure 1 depicts the 6 normalized time series whose average is M6. They all show a typical V-pattern with a maximum around the year 1800 AD, a fall until a minimum at about 1880 AD, and a rise until the recent maximum at about 2000 AD. Both maxima have similar magnitudes. Figure 2 gives M6 superimposed with IC showing the V-shape of the temperature history equally in the Northern and Southern Hemisphere, and therefore as a global phenomenon. We note that NH temperature reconstructions corroborate the temperature decrease in the 19th century (Crowley, 2000).

The time series M6 and SPA are analyzed by the discrete Fourier transform (DFT) with zero padding. Zero padding in the time domain increases the frequency steps and corresponds to an ideal interpolation in the frequency domain. To obtain information about the significance of the peaks, we adjoin in the DFT spectra the 90 % and the 95 % confidence limits of the background noise evaluated by Monte Carlo simulations. Next, an empirical reconstruction of M6 based on the results of a DFT

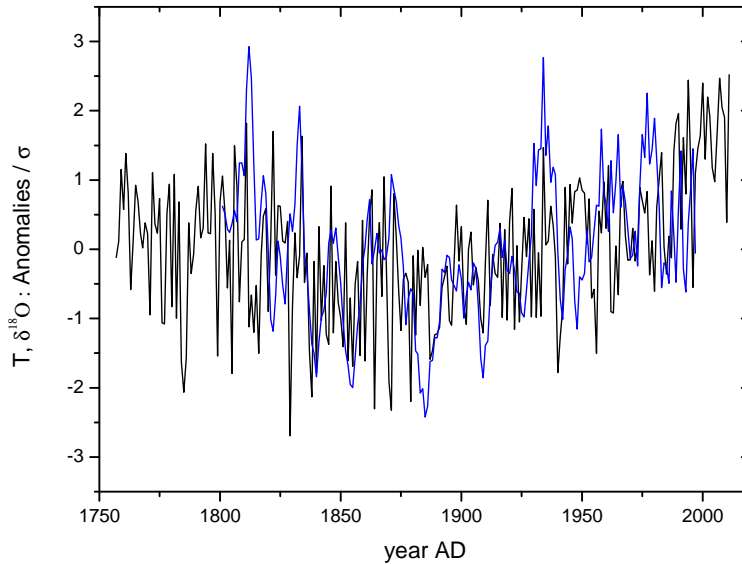


Fig. 2. (color online): Northern hemisphere (Central European) instrumental temperature averaged record M6 (black) together with the Antarctic ice core record IC (blue) as a SH counterpart, each as an anomaly divided by the standard deviation.

without zero padding is executed which is restricted to oscillations of periods not shorter than 30 yr.

45 Due to the quality of the reconstruction one can predict near future temperature changes as indicated in Figure 5.

2 The data basis

The instrumental records from Central Europe consist of monthly means and are continuous except for Paris and Munich which are made up each of two parts from different nearby stations. However,

50 both for Paris and Munich the major part of the two single time series covers nearly the whole record length. The monthly means are converted to yearly means for the application of the DFT. In contrast to this, both the stalagmite record SPA and the ice core record IC consist of yearly means. The details of the records used in this paper are: Kremsmünster, monthly (1768–2010) (Auer et al., 2007); Hohenpeissenberg, monthly (1781–2010) (CRU, 2012); Prague, monthly (1770–2010) (CHMI, 2012);
 55 Paris-Le-Bourget, monthly (1757–1993) (Météo France, 2012), Paris-Montsouris, monthly (1994–2011) (Météo France, 2012); Munich-Riem, monthly (1781–2007) (Auer et al., 2007), Munich-Airport, monthly (2007–2011) (DWD, 2012); Vienna, monthly (1775–2010) (CRU, 2012); Stalagmite record SPA, unequally yearly (–90–1935) (Mangini et al., 2005); Ice core record IC, yearly (1801–1997) (Graf et al., 2002).

60 3 Methods

In the literature, several methods for the spectral analysis of time series are reported (Ghil et al., 2002). We used in this study the simple method of the discrete Fourier transformation (DFT). The time series M6 has equal time steps of one year and, therefore, the DFT can be applied without any further complications. However, for SPA which has unequal time steps the DFT requires an
 65 interpolation procedure in the time domain. With the data f_k in the time domain and N as the number of f_k (here $N = 254$) the DFT is

$$F_j = \frac{1}{N} \sum_{k=0}^{N-1} f_k W_N^{-kj} \quad (1)$$

with $W_N = e^{2\pi i/N}$ and the reverse transformation

$$f_k = \sum_{j=0}^{N-1} F_j W_N^{kj} \quad (2)$$

70 In principle, for unequal time steps the DFT is not applicable. Interpolation in the time domain, however, can result in enhancing the low frequencies and reducing the high frequency components (Schulz and Mudelsee, 2002). Therefore, we compared in a first step the result of the interpolated SPA record yielded by DFT with the result of the unmodified SPA record yielded by the Lomb-Scargle periodogram method. As an outcome, no significant differences in the peak frequencies but
 75 differences in the peak strengths occur between DFT with the interpolated SPA and the periodogram with the unchanged SPA. Because the stalagmite record SPA is predominantly used in this paper for a comparison of frequencies with M6 and because the widest time steps of SPA lie in the period from 90 BC until 500 AD, we omitted the first years of 90 BC until 500 AD and carried out again the comparison of the DFT with the periodogram. As a result, we find for the shortened interpolated
 80 SPA both for the frequencies and the power densities good accordance of the DFT and the periodogram. To obtain more frequency steps we generally applied zero padding in the DFT except for the empirical reconstruction of M6. Furthermore, the power values F_j in Eq. (1) were normalized by the area below them.

In order to obtain confidence levels of the background noise, the autocorrelation (persistence) of
 85 the records M6 and SPA has to be considered. The appropriate method for the evaluation of the persistence of a time series is the detrended fluctuation analysis (DFA) specified in (Kantelhardt, 2004), (Lennartz and Bunde, 2009, 2011) and references cited therein. In general, one visualizes the significance of peaks in DFT power spectra against the background noise with lines of 90 %, 95 % or 99 % confidence levels and assumes a background of red noise as an AR1 process (Schulz and
 90 Mudelsee, 2002). We applied a more realistic procedure that accounts for the autocorrelation of the record: The autocorrelation (persistence) of a time series is characterized by its Hurst exponent α which can be evaluated with DFA. For the stalagmite record SPA an α of 0.9 was already reported (Lüdecke, 2011), which indeed corresponds roughly to a red noise background. However, our DFA

analysis of M6 yielded a value of $\alpha = 0.58$. Because the DFA needs a minimum of 500 data points
95 for the autocorrelation analysis of M6 the monthly mode of M6 had to be applied. To eliminate seasonal influences, we subtracted the seasonal mean value from the data and divided by the seasonal standard deviation. This yields a normalized record without seasonal effects that is appropriate for the DFA (Lennartz and Bunde, 2009). The result of $\alpha = 0.58$ corresponds to other values for temperature series (Rybski and Bunde, 2009) and demonstrates that red noise as a background for M6
100 is not adequate. Therefore, one has to ascertain that the random records of the Monte-Carlo method simulating the background noise have the appropriate α values. For this purpose we generated surrogate records with the Hurst exponents $\alpha = 0.9$ for SPA and $\alpha = 0.58$ for M6 by using a standard method (Turcotte, 1997).

The DFT without zero padding was applied for the reconstruction of M6 (Eqs. 1, 2). Here, we
105 chose the basic method of selecting specific frequencies for the reverse transformation (Eq. 2) resulting directly in the reconstruction without any further optimization procedures. Choosing among the first 8 frequencies of the DFT which corresponds to all periods not shorter than 30 yr (definition of "climate" as 30 yr temperature average) the 6 with the highest power density yields an excellent reconstruction of M6. No other spectral contributions were used.

110 4 DFT and Wavelet analysis

The results of the DFT are shown in Figure 3. The left panel of Fig. 3 depicts the power densities of the DFT for M6 with padded zeros together with the 90 % and 95 % curves of confidence yielded by the Monte Carlo simulations. The right panel shows the same for SPA. Figure 4 shows the wavelet spectrum for the interpolated stalagmite record SPA. For M6 a wavelet analysis is meaningless because of the shortness of the time series. Four of our six selected frequencies in M6 have
115 a confidence level over 95 % and only one over 99 %. A rather good agreement of the frequency peaks between M6 and SPA exists for the periods of (roughly) 250, 80, 65, and 35 yr. A conspicuous disagreement is found for the peak with the period of 100 yr which is very strong in SPA and nearly lacks in M6.

We note that the 250 yr peak in Fig. 3 left results from only about one 250 yr period, which covers
120 the entire record length. This is clearly insufficient to detect real oscillatory dynamics. The question thus, if there is in fact a 250 yr periodicity, can only be decided by longer records. Fortunately the SPA record covers about 2000 yr. Its strong peak at ~ 235 yr (Fig. 3 right) shows that a periodicity of this length is real. Its phase is matching well with SM6. This is evidence that the 250 yr peak in Fig.
125 3 left is not an artefact and corresponds to a real oscillation. The wavelet diagram shows that this cycle has been the dominant one since about 1100 AD (see Fig. 4) corresponding to the dominant strength of this cycle in M6.

The wavelet analysis (Fig. 4) shows that historically a 125 yr cycle was dominating the earth

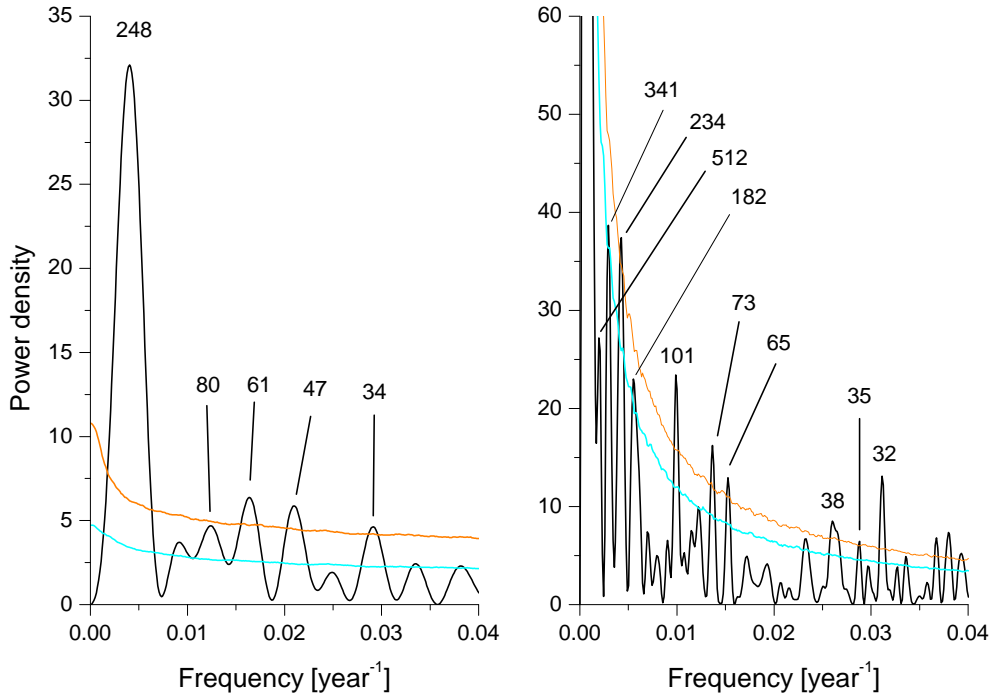


Fig. 3. (color online) Left panel: DFT of M6 (average from 6 central European instrumental time series). Right panel: same for SPA, interpolated time series of a stalagmite from the Austrian Alps for the period 500 - 1935 AD. In both DFT analyses the records were padded with zeros. The upper confidence curve (brown) is for 95%, the lower (cyan) for 90% against background noise, each of those established by 10,000 Monte Carlo runs. The most relevant peaks are indicated by their period length.

temperature. During the many decades this cycle has weakened and the strength shifted to the subharmonic (see discussion) of 250 yr, which is now the dominant periodicity. In addition, the 4 lowest frequencies in Fig. 3 (right) show rather precisely the spectral pattern of the generation of the subharmonics (1, 0.5, 0.75, 1.25, which correspond to the evaluated periods 234, 512, 341, 234 yr). Such subharmonic generation is characteristic for the transition from periodic to chaotic oscillations of dynamic systems (Feigenbaum, 1978, 1983).

135 5 Empirical reconstruction of the mean record M6

Our empirical reconstruction of M6 (hereafter RM6) with $N = 254$ data points is based on the DFT without zero padding (Eq. 1). For the inverse transformation (Eq. 2) we selected empirically 6 periods (frequencies > 0) obeying the conditions that they are longer than 30 yr and yield the strongest power densities among the first 8 DFT-frequencies i/N , $i = \{1, \dots, 8\}$. As a result, the

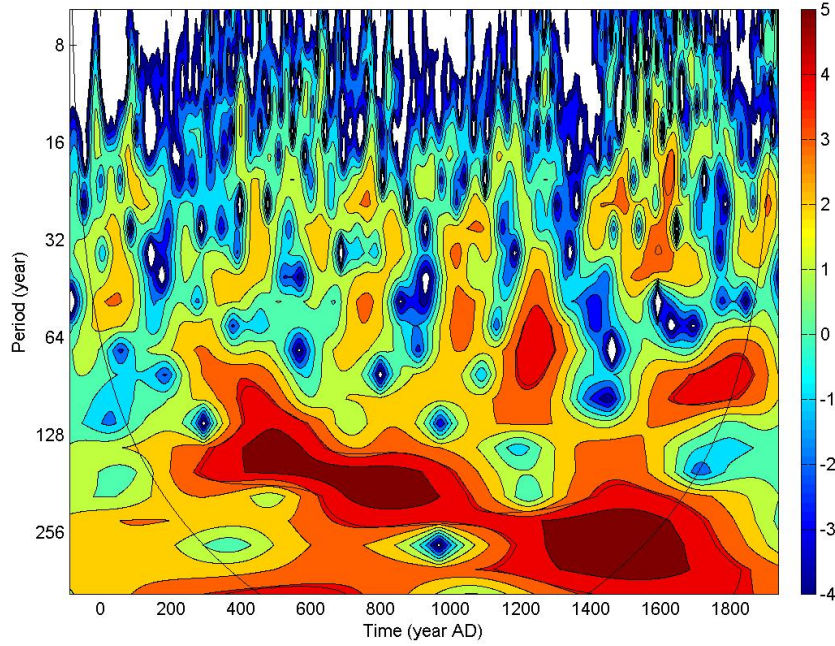


Fig. 4. (color online) Wavelet (Morlet) spectrum (Torrence and Compo, 1998), (Torrence and Compo, 2012) of the interpolated SPA record for the period -90 until 1935 AD. The solid black line from the left to the right top of the Figure is the cone of influence (below the coi the results are not significant). The spectrum shows that the power density transfers with time from the 128 yr cycle to the 256 yr cycle (period doubling).

140 reconstruction is:

$$f_k = \sum_j F_j W_N^{kj} \quad j = 0, 1, 3, 4, 5, 6, 7 \quad (3)$$

$$RM6(t) = \sum_j a_j \cos(2\pi jt/N) + b_j \sin(2\pi jt/N) \quad j = 0, 1, 3, 4, 5, 6, 7 \quad (4)$$

The parameters of Eq.(4) are given in Table 1. Figure 5 depicts the comparison of the reconstruction RM6 and the record M6 after being boxcar-smoothed over 15 yr (hereafter SM6).

145

6 Confidence level of the reconstruction

The Pearson correlation of the smoothed record SM6 with the reconstruction RM6 (black and red curves in Fig. 5) has a value of $r = 0.961$. In order to ascertain the statistical confidence level of this accordance, we assumed a null hypothesis and evaluated it by Monte Carlo simulations based on random surrogate records of the same length and the same Hurst exponent ($\alpha = 0.58$) as M6

Table 1. Frequencies, periods, and the coefficients a_j and b_j of the reconstruction RM6 due to Eqs. (1), (3), and (4) ($N = 254$).

j	j/N (yr^{-1})	Period (yr)	a_j	b_j
0	0	–	0	0
1	0.00394	254	0.68598	–0.12989
2	0.00787	127	–	–
3	0.01181	85	0.19492	–0.14677
4	0.01575	64	0.17465	–0.22377
5	0.01968	51	0.14730	–0.10810
6	0.02362	42	–0.02510	–0.12095
7	0.02756	36	0.12691	0.01276
8	0.03150	32	–	–

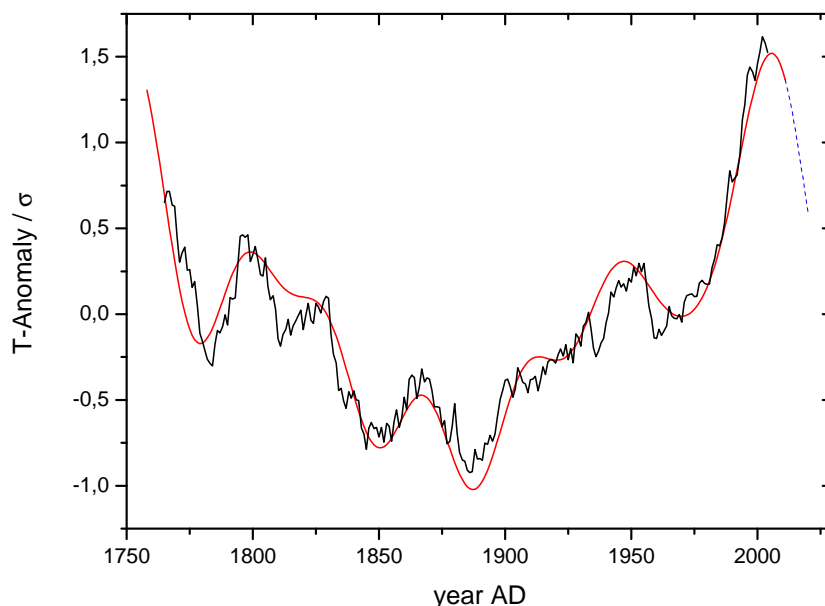


Fig. 5. (color online) 15 year running average record SM6 (black); reconstruction RM6 according to Eq.(1), Eq.(3), Eq.(4) (red); projection of future NH temperatures mainly to the ~ 65 yr periodicity (dashed blue).

generated by a standard method (Turcotte, 1997) (the surrogate records hereafter SU, and the boxcar-smoothed SU over 15 yr hereafter SSU). As the null hypothesis we assumed that the accordance of the reconstruction RM6 with SM6 is caused by chance. We applied 10 000 surrogate records
155 SU. Each of the record was analyzed following the same procedure as for M6. Next, for each surrogate SU the reconstruction was generated that used – again following the procedure as for M6 – 6 frequencies with the strongest power densities among the first 8 frequencies of the DFT without

zero padding. Finally, the Pearson correlation of this reconstruction with SSU was evaluated. As a result, among 10 000 SU we found one surrogate record with the maximal $r = 0.960$, 9 records with $r \geq 0.95$ and 53 records with $r \geq 0.94$. Therefore, the null hypothesis could be rejected with a confidence level of $> 99.9\%$.

7 Discussion

The temperature records from 6 Central European stations show remarkable agreement, justifying their averaging to produce a “Central European temperature record” M6. The characteristic of these records, namely the pronounced minimum around 1880 is equally found in Antarctic ice core temperature data, which are also overall in agreement with M6, revealing this 1880 minimum as a global phenomenon.

The Fourier transform of M6 yields pronounced spectral peaks, indicating dynamics by periodicity. Indeed, the reconstruction, in which nothing but the 6 strongest frequency components (with periods > 30 yr) are retained, yields excellent agreement with the measurement M6. A temperature record obtained from a Central European stalagmite is also Fourier-analyzed, and shows, for comparison, similar periodicities. It confirms the 250 yr period yielded by the DFT of M6 as a real and dominant oscillation. The cause of the periodicities is not known to us. We would think that they constitute intrinsic system dynamics as it is generally found for dissipative systems with energy input (here the Earth dissipating the radiative energy provided by the Sun). Such dynamics are the physics behind all terrestrial weather dynamics (e.g. trade winds or El Niño). This interpretation as intrinsic system dynamics is supported by the wavelet analysis of the stalagmite data. The latter shows a drift over 1600 yr of peak intensity from the 128 yr period to the 256 yr period. A further doubling to ~ 500 yr (peak visible in the spectrum, right Fig. 3) causes the recent weakening of the 250 yr period, visible in the wavelet diagram. Such a shifting of energy from a fundamental to a subharmonic frequency component is characteristic of the Feigenbaum universal scenario of transition to chaos by a cascade of subharmonics, for nonlinear, driven, dissipative systems (Feigenbaum, 1978, 1983). Whereas harmonic generation is just an expression of nonlinearity, subharmonic generation is peculiar to the Feigenbaum scenario, since it requires, different from harmonic generation, a particular phase-matching mechanism for sum- and difference-frequencies generated by the system non-linearities. The 4 lowest frequency lines of Fig. 3 (right) give additionally evidence of the climate oscillations as intrinsic dynamics. They show the pattern characteristic of generation of two subharmonics which corresponds rather convincingly to the Feigenbaum transition to Chaos. Such a transition requires the continuous, monotonic change of a “control parameter”. The world temperature which is recently found to drop continuously over the last 2000 yr (Esper et al., 2012), may well have the role of “control parameter” here.

The agreement of the reconstruction of the temperature history using only the 6 strongest compo-

nents of the spectrum, with M6, shows that the present climate dynamics is dominated by periodic processes. The prediction of a temperature drop in the near future results essentially from the ~ 64 yr cycle, which to our knowledge is the Atlantic-(Pacific-) Multidecadal Oscillation. 4 periods of the 64 yr cycle are clearly visible in Fig. 5 and the A-P-Multidecadal Oscillations can be traced back for more than 1000 years. This cycle was identified by (Schlesinger , 1994) as intrinsic dynamics. (Tsonis , 2007) found a mechanism in observed climate indices of the period 1900-2005, which is consistent with the theory of synchronized chaos. On the other hand external causes for periodic dynamics exist also, such as planetary motion, solar cycles and atmosphere-ocean-sea ice interaction (Scafetta, 2012a,b,c; Sollheim et al., 2012; Dima , 2007).

Appendix A

Abbreviations of the time series in this paper

IC	Ice core record as yearly $\delta^{18}\text{O}$ values.
M6	Mean of 6 instrumental records in Central Europe (both monthly and yearly).
RM6	Reconstruction of M6.
SPA	Stalagmite time series as yearly temperatures yielded by interpolation.
SM6	M6 smoothed over 15 yr (boxcar).
SU	Surrogate records with Hurst exponents $\alpha = 0.58 \pm 0.3$.
SSU	Smoothed SU over 15 yr (boxcar).

Acknowledgements. We thank Régine Larrieu (météo france, Toulouse) for kindly allocating the Paris time series for our studies. We thank Luboš Motl for his technical information about the Prague record.

References

- Auer, I., Böhm, R., Jurkovic, A., Lipa, W., Orlik, A., Potzmann, R., Schöner, W., Ungersböck, M., Matulla, C., Briffa, K., Jones, P., Efthymiadis, D., Brunetti, M., Nanni, T., Maugeri, M., Mercalli, L., Mestre, O., Moisselin, J.-M., Begert, M., Müller-Westermeier, G., Kveton, V., Bochnicek, O., Stastny, P., Lapin, M., Szalai, S., Szentimrey, T., Cegnar, T., Dolinar, M., Gajik-Capka, M., Zaninovic, K., Majstorovic, Z., and Nieplova, E.: HISTALP – historical instrumental climatological surface time series of the Greater Alpine Region, *Int. J. Climatol.*, 27, 17–46, 2007.
- 210 Czeck Hydrometeorological Institute, 143 06 Praha 4 Czech Republic, available at: <http://zmeny-klima.ic.cz/klementinum-data/> (last access: August 2012), 2012.
- Climatic Research Unit (CRU), University of East Anglia (UK), available at: www.cru.uea.ac.uk/cru/data/temperature/station-data/ (last access: August 2012), 2012.
- Deutscher Wetterdienst (DWD), Frankfurter Straße 135, 63067 Offenbach (Germany), available at: www.dwd.de (last access: August 2012), 2012.
- 220 Esper, J., Frank, D. C., Timonen, M., Zorita, E., Wilson, R. J. S., Luterbacher, J., Holzkämper, S., Fischer, N., Wagner, S., Nievergelt, D., Verstege, A., and Büntgen, U.: Orbital forcing of tree-ring data, *Nat. Clim. Change*, in press, doi:10.1038/NCLIMATE1589, 2012.
- Feigenbaum, M. J.: Quantitative universality for a class of nonlinear transformations, *J. Stat. Phys.*, 19, 25–51, 1978.
- 225 Feigenbaum, M. J.: Universal behavior in nonlinear systems, *Physica D*, 7, 16–39, 1983.
- Ghil, L., Allen, M. R., Dettinger, M. D., Ide, K., Kondrashov, D., Mann, M. E., Robertson, A. W., Saunders, A., Tian, Y., Varadi, F., and Yiou, P.: Advanced spectral methods for climatic time series, *Rev. Geophys.*, 40, 1–41, 2002.
- 230 Graf, W., Oerter, H., Reinwarth, O., Stichler, W., Wilhelms, F., Miller, H., and Mulvaney, R.: Stable-isotope records from Dronning Maud Land, Antarctica, *Ann. Glaciol.*, 35, 195–201, 2002.
- Kantelhardt, J. W.: *Fluktuationen in komplexen Systemen*, Habilitationsschrift, Universität Gießen, Germany, 19 June, available at: www.physik.uni-halle.de/Fachgruppen/kantel/habil.pdf (last access: August 2012), 2004.
- 235 Lennartz, S. and Bunde, A.: Trend evaluation in records with long-term memory: application to global warming, *Geophys. Res. Lett.*, 36, L16706, doi:10.1029/2009GL039516, 2009.
- Lennartz, S. and Bunde, A.: Distribution of natural trends in long-term correlated records: a scaling approach, *Phys. Rev.*, E84, 021129, doi:10.1103/PhysRevE.84.021129, 2011.
- Lüdecke, H.-J.: Long-term instrumental and reconstructed temperature records contradict anthropogenic global warming, *Energy & Environment*, 22, 723–745, 2011.
- 240 Mangini, A., Spötl, C., and Verdes, P.: Reconstruction of temperature in the Central Alps during the past 2000 years from a ¹⁸O stalagmite record, *Earth Planet. Sc. Lett.*, 235, 741–751, 2005.
- Météo France: 42 Av. Gaspard Coriolis, 31057 Toulouse Cedex (France), 2012.
- Rybski, D. and Bunde, A.: On the detection of trends in long-term correlated records, *Physica A*, 388, 1687–1695, 2009.
- 245 Schulz, M. and Mudelsee, M.: REDFIT: estimating red-noise spectra directly from unevenly spaced paleoclimatic time series, *Comput. Geosci.*, 28, 421–426, 2002.

- Torrence, C. and Compo, P.: A practical guide to wavelet analysis, *B. Am. Meteorol. Soc.*, 79, 61–78, 1998.
- Torrence, C. and Compo, P.: Wavelet software, available at: <http://atoc.colorado.edu/research/wavelets/> (last
250 access: August 2012), 2012.
- Turcotte, D. L.: *Fractals and Chaos in Geology and Geophysics*, 2nd Edition, Cambridge University Press, Cambridge, 1997.
- Scafetta, N.: Testing an astronomically based decadal-scale empirical harmonic climate model versus the general circulation climate models, *J. Atmospher. Sol. Terr. Phys.*, 80, 124–137, 2012
- 255 Scafetta, N.: Multi-scale harmonic model for solar and climate cyclical variation throughout the Holocene based on Jupiter-Saturn tidal frequencies plus the 11-year solar dynamo cycle, *J. Atmospher. Sol. Terr. Phys.*, 80, 296–311, 2012
- Scafetta, N.: Does the Sun work as a nuclear fusion amplifier of planetary tidal forcing? A proposal for a physical mechanism based on the mass-luminosity relation, *J. Atmospher. Sol. Terr. Phys.*, 81-82, 27–40,
260 2012
- Sollheim, J.-E., Stordahl, K., Humlum, O.: The long sunspot cycle 23 predicts a significant temperature decrease in cycle 24, *J. Atmospher. Sol. Terr. Phys.*, 80, 267–284, 2012
- Crowley, T.J.: Causes of Climate Change Over the past 1000 Years, *Science*, Vol. 289, 270–277, 2000
- Dima, M. and Lohmann, G.: A Hemispheric Mechanism for the Atlantic Multidecadal Oscillation, *J. Climate*,
265 Vol. 20, 2706–2719, 2007
- Schlesinger, E. and Ramankutty, N.: An oscillation in the global climate system of period 65-70 years, *nature*, Vol. 367, 723–726, 1994
- Tsonis, A.A., Swanson, K., and Kravtsov, S.: A new dynamical mechanism for major climate shifts, *Geophys. Res. Lett.*, 34, L13705, doi:10.1029/2007GL030288, 2007